Front. Phys. China (2006) 3: 275－282
DOI 10.1007/s11467-006-0036-6

REVIEW ARTICLE

HU Zhan, JIN Ming-xing, XU Xue-song, CHENG Xi-hui, DING Da-jun

Acetone: isomerization and aggregation

Abstract The advanced experimental and theoretical techniques enable us to obtain information on the rearrangement of atoms or molecules in a reaction nowadays. As an example, we report on our research work on acetone isomerization and aggregation to give an insight into the reaction pathways, the products and their structures, and the growth regularity of aggregation. The evidences on the structural change of acetone and the stability of acetone clusters are found by a laser ionization mass spectrometer and the results are interpreted from theoretical analysis based on the DFT/B3LYP method. Various isomerization channels of acetone have been established and the optimal structures of the neutral clusters $(CH_3COCH_3)_n$ and the protonated acetone clusters $(CH_3COCH_3)_n H^+$ for n=1–7 have been determined.

Keywords isomer, cluster, acetone, chemical dynamics

PACS numbers 33.15.Hp, 82.30.Qt, 36.40.-C

1 Introduction

Studies on molecular reaction dynamics is one of most active areas in modern atomic and molecular physics, especially when advanced tunable light sources, such as lasers or synchrotron radiation, and well-developed computation techniques are employed [1－3]. The main aim of such studies on molecular reaction dynamics is to understand the process in a level of atoms and molecules and then try to better control the reaction. The questions to be answered are which bond is broken up or formed in a certain condition and what products are formed in a specific reaction from the point of view of energy states or potential surfaces of the chemical entireties involved [4, 5]. Because acetone acts as an excellent model for a class of organic molecules (ketone), its reaction and spectroscopy are of much interest and have been studied by numerous groups [6－9]. Also, acetone is one of the main air pollution products. Therefore, it is important to understand the photochemical process of acetone and acetone clustering in possible aerosol processes [10].

Different techniques have been employed in the studies of acetone unimolecular reaction such as dissociation, ionization, and isomerization. The early work includes electron impact ionization and decomposition [11, 12], UV dissociation and ionization [13, 14]. Combined with spectroscopic studies [15], the studies have provided many data for the energetics of acetone unimolecular reactions. Recently, Wei *et al*. [16] used a synchrotron radiation for investigating the photoionization and dissociation of acetone and various dissociation channels were established in a photon energy region of 8－20 eV.

As far as the isomerization processes of acetone are concerned, Zhang *et al*., in an electron bombardment experiment, showed that a small fraction of *A* state of acetone radical cation may rearrange to propen-2-ol, the enol form of acetone, through a scheme of acetone$^+$ ↔ 1, 2-epoxypropane$^+$ ↔ propen-2-ol$^+$ [17]. Majumder *et al*. provided another evidence for partial isomerization of the keto form to the enol form [18]. In their time-of-flight mass spectrometry ionized by a 355 nm ns-laser, the peaks at m/e = 29 (COH^+) in the case of CH_3COCH_3 and at m/e=30 (COD^+) for CD_3COCD_3 are shown up, which cannot be obtained through a simple dissociation of acetone. All these experiments suggest that, prior to decomposition, acetone can go through a process of the isomerization, resulted from the incomplete randomization of the excited energy in the molecules, which is in agreement

HU Zhan, JIN Ming-xing, XU Xue-song, CHENG Xi-hui, DING Da-jun (✉)
Institute of Atomic and Molecular Physics, Jilin University, Changchun 130012, China
E-mail: dajund@mail.jlu.edu.cn

XU Xue-song
The present address: Dalian Maritime Univeristy, Dalian 116026, China

Received April 4, 2006

with the early suggestion of non-ergodic process by Lifshitz and Tzidony [19].

Acetone clustering has been observed in supersonic molecular beams by various studies [7, 20—23]. Buzza *et al*. measured the time-of-flight mass spectra of acetone clusters and their fragments such as $[(CH_3)_2CO]_n^+$, $[(CH_3)_2CO]_{n-1}CH_3^+$, $[(CH_3)_2CO]_{n-1}CH_3CO^+$ ($n = 1-4$) by using a femtosecond laser ionization of acetone molecular beam [22]. These fragments were believed to have come from the dissociation of the larger clusters [23]. Donaldson *et al*. interpreted the influence of acetone clustering on the coupling, energies and lifetime of the molecular states by comparing the absorption spectra of acetone molecules and clusters [7]. For small acetone clusters ($n \leqslant 3$), the structures have also calculated by either a semi-empirical or quantum method [24, 25].

In this article, we summarize the recent work on isomerization and aggregation of acetone molecules. Our studies show that acetone molecules have several isomer structures that can be realized by photoinduced processes and the molecular clusters can be formed even in a unimolecular condition of a supersonic molecular beam. Comparing with the theoretical calculation from a quantum ab initio approach of density function theory (B3LYP/DFT), the detailed information on the isomerization and clustering of acetone molecules is obtained such as the reaction pathways and products, the growth regularity and the stable structures of the clusters. The results derived is suggestive and of general interest for organic molecules.

2 Experimental methods

The experimental system contains a laser, a time-of-flight massz spectrometer (TOF-MS) with a reflection, a gaseous mixing system, and a data acquisition system. Quanta-Ray Nd^{3+}: YAG laser generates 355 or 266 nm UV laser pulse with about 8 ns pulse duration and 10 Hz repetition rate. After passing through a quartz lens with 25 cm focal length, the resulting laser intensity is variable from 10^7 W/cm^2 to 10^{10} W/cm^2. This laser beam is focused and directed into the TOF mass spectrometer. It is intersected perpendicularly with a molecular beam of acetone from a supersonic jet expansion. Multiphoton ionization is generated and the produced ions are accelerated and fly in the direction perpendicular both to the laser and the molecular beams. Ion reflector is used in TOF-MS for reducing possible initial energy and spatial influences on the mass resolution. The ions are measured by a dual microchannel plate detector after reflecting. The output ion signals then are amplified by a fast preamplifier (EG&G VT120), and sent to a picosecond time analyzer (EG&G 9308) or a digital oscilloscope (LeCroy 9361). The final spectrum is recorded and analyzed by a computer. By elaborate design of the reflectron, detector, transmitting line, and the potentials applied a mass resolution better than 3 000 has been achieved in the experiments. The molecular beam is formed by using a pulsed valve (General Valve Series 9) with a typical backing pressure of 3×10^5 Pa (92% Ar and 8% acetone vapor) and through a two-stage differential pumping. All timing and synchronization of the experimental setup are controlled by a delayed signal generator (SRS DG 535).

3 Theoretical calculations

A quantum ab initio calculation is used for the determination of structures and energies of the transition, intermediate, and final products in isomerization and cluster processes of acetone. The theoretical approach is based on density function theory (DFT), which has emerged as a useful tool for calculating the structures of larger systems, particularly when the local density approximation (LDA) for exchange and/or correlation is used [26, 27]. One of the DFT methods used frequently is the B3LYP method (the combination method of Becke's three parameters hybrid functional with Lee, Yang and Parr correlation functional) [28—30], with different levels of the standard basis sets, that can give an approach to treat the electron correlation and, therefore, predict molecular geometries reliably.

4 Isomerization of acetone

In our experiment [31], acetone molecule in a supersonic beam is irradiated by 266 nm and 355 nm laser, the obtained time-of-flight mass spectrum shows a series of minor peaks in the region of mass to charge ratio 24—31, as shown in Fig. 1 for 266 nm and (2) for 355 nm. For identifying these fragments, a deuterated sample was used for molecular beam. The obtained mass spectrum of deuterated acetone under the same condition is shown in Fig. 1 (3) and (4). Thus, the composition

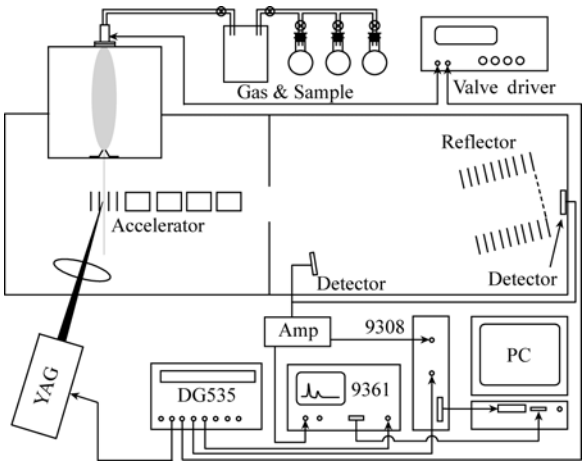

Fig. 1 Experimental setup of a laser ionization time-of-flight mass spectroscopy of molecular beam. It contains a laser, a time-of-flight mass spectrometer (TOF-MS) with a reflection, a gaseous mixing system, and a data acquisition system.

of peaks m/z=24, 25 and 26 in acetone spectrum can be determined to be C_2^+, C_2H^+ and $C_2H_2^+$. The composition of peak m/z = 29 in Fig. 2 (1), which can be COH^+ or $C_2H_5^+$, is determined by comparing the relative intensities of peaks 27, 29 and 31 in acetone spectra and 30, 34 in deuterated acetone spectra. In both 266 nm and 355 nm cases, the intensities of peaks m/z=34 in deuterated acetone spectra are very small, while the m/z=29 peaks in acetone spectra are in the middle intensity in the 266 nm case and the strongest intensity in the 355 nm case, so the m/z =34 peaks in deuterated acetone spectra cannot be corresponded to m/z=29 peaks in acetone spectra. Thus, the m/z = 30 peaks in deuterated acetone spectrums have two contributions, i.e., COD^+ and $C_2D_3^+$, corresponding to m/z = 27 (COH^+) and 29 ($C_2H_3^+$) in acetone spectrums. The ion COH^+ is from acetone's isomer 1-propen-2-ol or acetyl radical's enolic isomerization product CH_2 = COH. As generally been accepted by previous works [18, 32], the isomerization from acetone ion to 1-propen-2-ol ion is realized by a proton transfer from one of the methyl group to the O atom. Thus, the peaks of m/z = 34 in deuterated acetone spectrums are corresponding to peaks m/z =31 in acetone spectrums, indicating the ion of CH_3O^+.

The isomerization process from acetone to 1-propen-2-ol can be written as Fig. 3 (a). There are two acetone's isomers that can produce CH_3O^+ ion by fragmentation, allyl alcohol and methoxyethene. Considering their structures, it is proposed that they should be two-process isomerizations, involving a transient product of 1, 2-epoxypropane, the mechanism of which is shown in Fig. 3 (b, c), (b, d) and (b, e). Processes (c), (d) and (e) are the isomerization mechanisms of 1, 2-epoxypropane given by Dunikova *et al*. [33], while (b) is the reverse process of their study from 1, 2-epoxypropane to acetone.

To validate this proposal, we carried out a laser ionization mass spectroscopy of 1, 2-epoxypropane under 266 nm and 355 nm with the same laser intensity. The result is shown in Fig. 4. A clear peak of m/z = 31 indicates the existence of CH_3O^+ ion and illustrates that the process (c) or (d) or (e) is a major process. The similarity of the relative peak intensities of peaks m/z = 24–27, 31 in Fig. 2 with the above spectrum of Fig. 4 and Fig. 2 (2) with the below spectrum of Fig. 4 declares that these peaks in Fig. 2 are from acetone isomers and the isomerization process should involve a transient product of 1, 2-epoxypropane. Furthermore, $C_2H_n^+$ (n = 0–2) are believed to be the successive ionization/dissociation products of $C_2H_3^+$ ion from allyl alcohol or methoxyethene since, as it is seen from a test of varying laser intensity, the intensity of peak m/z = 27 increases with a decreasing of laser intensity.

Figure 5 shows a schematic illustration of the energies of the reactant, transient states, intermediates and the products of isomerization process (c), (d) and (e) [34]. From the overall barrier heights, it is seen that the process (c) and (d) are favorable than (e). As the overall barrier heights of (c) and (d) are close, considering each reaction step may have a reverse reaction competing with it, a process with only one step, i.e., the process (c) is more favorable than one with three steps, i.e., the process (d).

The detailed calculation was performed by Xu *et al*. [35]. The structures and frequencies of the reactant, intermediate isomers, transition states, and products were calculated at the B3LYP/6-31G (d, p) level of the DFT while the single-point energy calculations were obtained at the QCISD (T)/cc-pVDZ level using the B3LYP/6-31G (d, p) optimized geometries. The zero-point vibration energies (ZPVE) at the B3LYP/6-31G (d, p) level were also included and they were scaled by the ZPVE scaling factor of 0.980 6 [36]. To confirm the

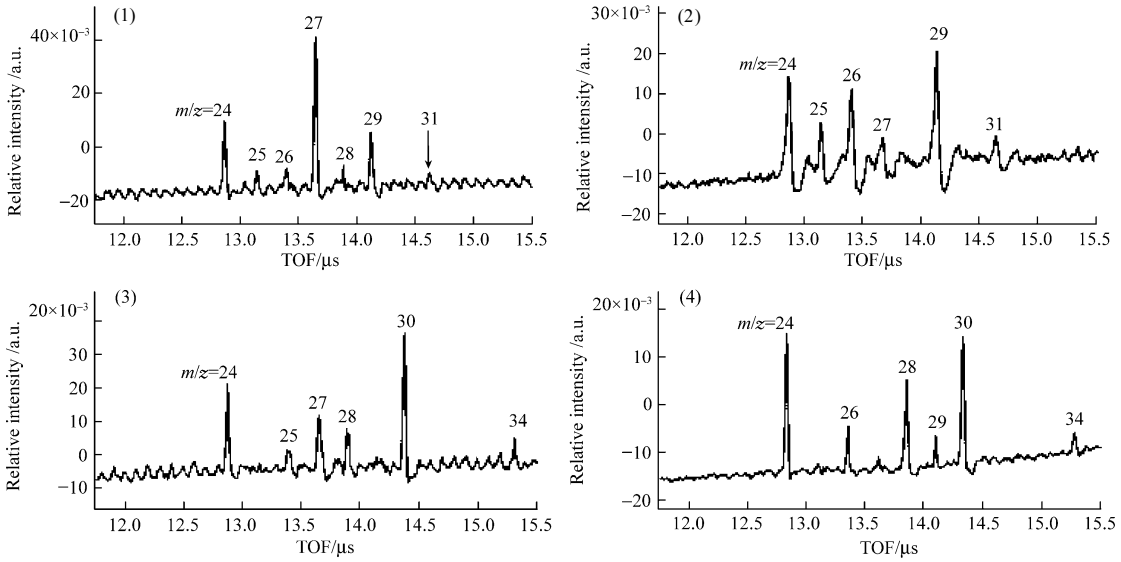

Fig. 2 TOF Mass spectra of acetone (**1**), (**2**), and deuterated acetone (**3**), (**4**). These mass spectra were obtained by a laser ionization with 266 nm [seeing (**1**), (**3**)] and 355 nm [seeing (**2**), (**4**)].

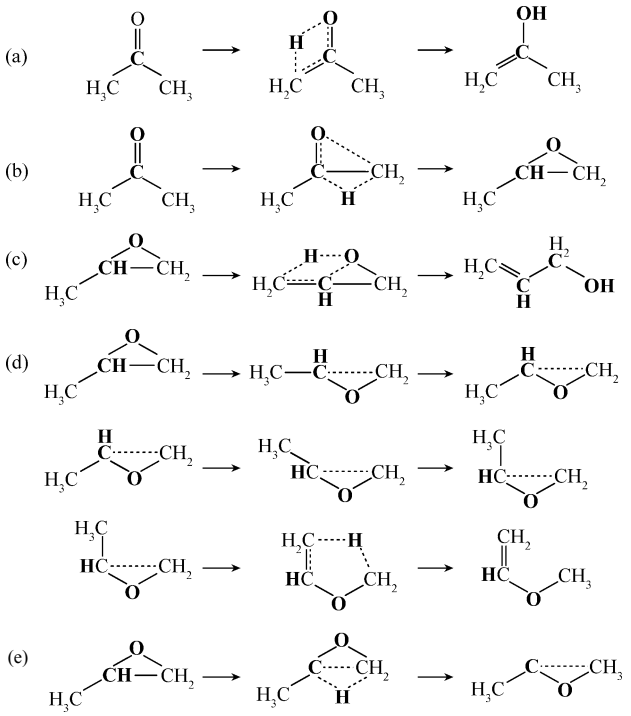

Fig. 3 Acetone isomerization processes for forming (**a**) 1-propen-2-ol, (**b**) and (**c**) allyl alcohol, (**b**) and (**d**) trans-methoxyethene, (**b**) and (**e**) *cis*-methoxyethene.

correction of the connection of the transition states with the reactants and products obtained, the intrinsic reaction coordinate (IRC) calculations were also carried out at the B3LYP/6-31G (d, p) level of the theory. Altogether five isomerization reaction channels are confirmed from this work by using the IRC method and the corresponding isomerization products are methoxyethene (*cis*- and *trans*-), allyl alcohol, and propen-2-ol. Among them, four channels are through 1, 2-poxypropane. Obviously, 1, 2-epoxypropane is an important intermediate in the isomerization process of acetone molecule. Judged by the number of transition states and the height of energy barriers, the reaction channel from acetone to allyl alcohol is preferable and allyl alcohol is inferred as the most feasible product among these four acetone isomers. Finally, it is noted that all the isomerization processes of acetone obtained in our work involve the process of proton transfer as in isomerization processes of many organic molecules. These studies help to give more insight into a large variety of similar molecules.

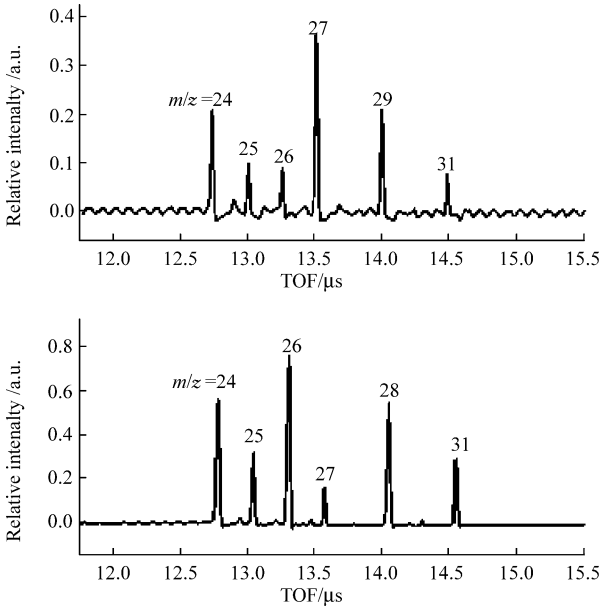

Fig. 4 Laser ionization mass spectrums of 1, 2-epoxypropane for comparison (above: by 266 nm, below: by 355 nm).

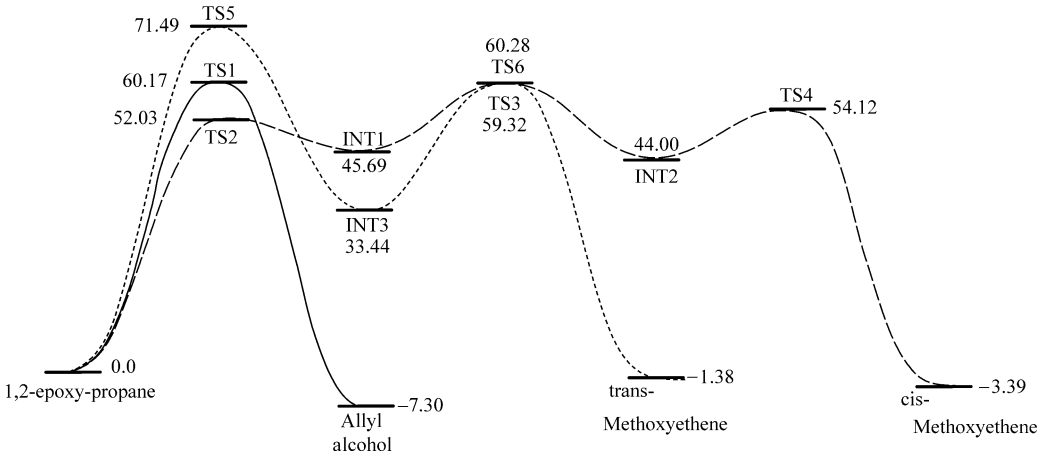

Fig. 5 Schematic diagram of the energetics for isomerizations of 1, 2-epoxypropane, as an important intermediate of acetone. The transition and intermediate states with their relative energies (in kcal/mol) were obtained from the B3LYP/DFT calculation.

5 Acetone Clustering

The studies of structures and formation of atomic and molecular cluster are important for understanding many processes in physics, chemistry, biology, and even fundamental process in life phenomena, since these can give ability to varying the number of atoms or molecules to show the structure and property evolution with the size of matter from an isolated gas-phase atom or molecule toward a bulk limit [37—44]. Most of experimental observation from a supersonic expansion of gaseous molecular beam gives the information of these cluster stability. The structures of these clusters can be calculated based on some theoretical models such as DFT, molecular dynamics simulation.

Hu *et al*. observed the clusters and their fragments containing up to 12 acetone molecules in a unimolecular condition of the supersonic molecular beam by laser (355 or 266 nm) ionization mass spectrometer as given in Fig. 6 [45]. The mass peaks consist mainly of $(CH_3COCH_3)_n H^+$ (denoted by A_n), $(CH_3COCH_3)_n CH_3CO^+$ (denoted by B_n) and $(CH_3COCH_3)_n CH_3^+$ (denoted by C_n) in Fig. 6. Since acetone cluster ions are weakly bonded as a van der Waals cluster, it is believed that the $(CH_3COCH_3)_n CH_3CO^+$ and $(CH_3COCH_3)_n CH_3^+$ are formed from the dissociation of $(CH_3COCH_3)_{n+i}^+$ clusters, like in the case of acetone molecule. This can be taken as the evidence to illustrate why the parent cluster ions are rare to be observed in the mass spectra. Comparatively, the intense peaks of $(CH_3COCH_3)_n H^+$ observed suggest that the protonated cluster ions are more stable in the experimental condition. This result is in agreement with the general observation in the ionization process of weak bound cluster systems [46—49].

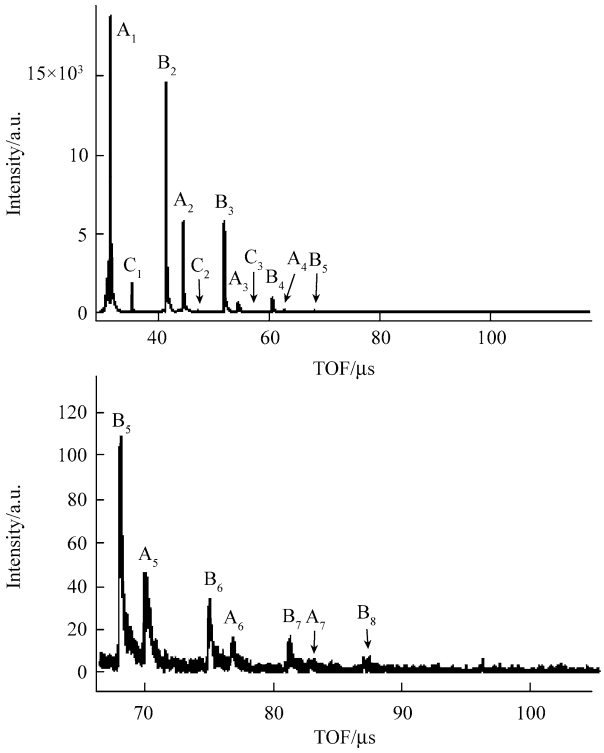

Fig. 6 The mass spectra of acetone molecular beam ionized by a nanosecond 355 nm laser (1×10^9 W/cm^2). The peaks denoted by A_n, B_n and C_n are $(CH_3COCH_3)_n H^+$, $(CH_3COCH_3)_n CH_3CO^+$ and $(CH_3COCH_3)_n CH_3^+$, respectively, and here n is the number of acetone molecules involved in cluster.

Lee *et al*. have calculated the structures of $(CH_3COCH_3)_n H^+$ (n = 1, 2), and they imposed C2 symmetry limitation when n = 2 [24]. Aviyente and Vernali used a PM3 semi-empirical method to calculate the structures of $(CH_3COCH_3)_n H^+$ ($n\leqslant3$) [25]. We have carried out a quantum chemical ab initio calculation to determine the structures of these acetone clusters with n = 2–7 [45, 50—52]. The initial geometries of these clusters are fully optimized at the B3LYP/DFT. The complete geometry optimization is performed by a Berny's optimizing algorithm [53] for the clusters on their ground state. Stationary points are confirmed through the calculation of vibrational frequencies. In general, the *ab initio* calculated frequencies are usually larger than the corresponding experimental values and contain known systematic errors due to the neglect of anharmonicity and electron correction [54]. Therefore, it is usually to scale frequencies predicted at the B3LYP/6-31G (d) level including some of the effects of electron correlation by empirical factor of 0.9613 [55].

The structures of the neutral clusters are determined by the energy-minimum criterion and frequency analysis. In order to find a local minimum of the energy with a sufficiently high probability, various initial structures for each cluster have been calculated. For the clusters $(CH_3COCH_3)_n$ with n = 2—7, the calculation and analysis show that the most stable clusters are with a ring-like structure, similar to that in the case of water clusters obtained by Xantheas and Dunning [56]. We show three stable structures, ring-like, end-to-head and compact chain, of the cluster $(CH_3COCH_3)_3$ in Fig. 7 as an example. The binding energies for these structures of the cluster are calculated, leading to the values of 0.074, 0.043 and 0.015 eV for the ring-like, end-to-head and compact chain structure of the cluster, respectively. Thus, the most stable cluster is the one with a ring-like structure among these three possible structures of the clusters.

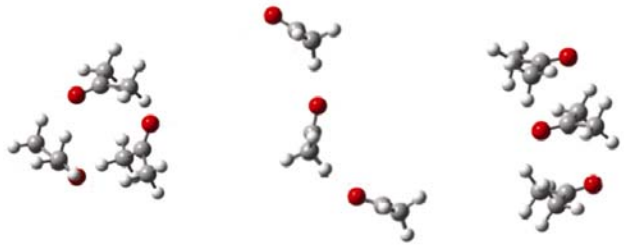

Fig. 7 Three stable structures of cluster $(CH_3COCH_3)_3$, calculated by DFT approach at the UB3LYP/3-21G (d) level. From the left to right: ring-like, end-to-head and compact chain structure. The most stable structure is the ring-like one.

For the stable structure of a neutral acetone molecule cluster $(CH_3COCH_3)_n$ with n = 1—7, the proton affinity was determined from the calculation [51], as listed in Table 1. The result shows that the proton affinity increases with increasing the cluster size. We consider that a proton, H^+, could act

as a bridge through its interaction with two oxygen atoms of different acetone molecule, since oxygen atom has the highest electronegativity among all atoms in acetone. The calculation generates some results in agreement with this consideration [57]. As seen in the most stable structures of $(CH_3COCH_3)_2H^+$ given in Fig. 8, the proton is attached on the oxygen atom for $(CH_3COCH_3)H^+$ and lies between two oxygen atoms for $(CH_3COCH_3)_2H^+$. The calculation at the UB3LYP/3-21G (d) level produces the structural parameters of $(CH_3COCH_3)_nH^+$ with $n = 1, 2$, which are listed in Table 2 together with the other results from different calculations [40, 41]. Our results have large improvement for the cluster of $n = 2$ since the method we used considers more complete geometry optimizations with larger basis set and includes the effects of electron correlation in the case of these small clusters.

Table 1 The proton affinity E_a of the neutral clusters calculated in their ring-like stable structures (in the unit of Hartree) .

N	1	2	3	4	5	6	7
E_a	0.3111	0.3594	0.3664	0.3742	0.3816	0.3834	0.3844

For larger protonated clusters, the calculated results show that cluster growth has certain regularity. It is interesting to note that the stable cluster $(CH_3COCH_3)_2H^+$, shown in Fig. 8, plays a kernel role, which can be regarded as an inner solvation shell in acetone clustering. Since $(CH_3COCH_3)_2H^+$ has several activated sites such as the methyl and middle carbon atoms, the coming acetones will attack them from different directions during the clustering. For example, the calculated results show that during acetone cluster growth, the third and fourth acetone molecules attack the central carbon atom of one of the acetone molecules in the inner shell $(CH_3COCH_3)_2H^+$, respectively, and when the size of the cluster becomes even larger, the coming acetones begin to attack the different sites in the inner shell, for example, the fifth acetone attacks the middle carbon atom of another acetone in the inner shell, the sixth and the seventh acetone molecules attack the two methyl of this acetone from almost opposite orientation. It can be expected that the successive acetone molecules will attack the methyl of the first acetone in the inner shell from the opposite direction to form $(CH_3COCH_3)_nH^+$ when $n = 8$ and 9, and so on, Finally, the protonated clusters with different sizes are formed (see Fig. 9). This regularity of the $(CH_3COCH_3)_nH^+$ cluster growing is similar as described in Ref. [58].

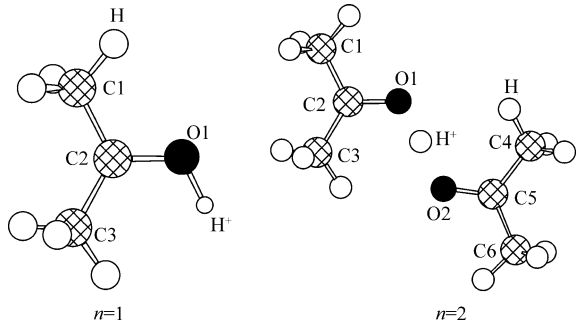

Fig. 8 The structures of $(CH_3COCH_3)_nH^+$ (n = 1, 2), calculated by DFT approach at the UB3LYP/3-21G (d) level.

Table 2 The structure parameters for $(CH_3COCH_3)_nH^+$ (n = 1, 2) shown in Fig. 8 obtained from a DFT calculation [57].

	n=1				n=2	
	Our work	HF / 6-31+G++[a]	MP2 / 6-31+G++[a]	PM3[b]	Our work	PM3[b]
Bond length / (0.1 nm)						
C1–C2	1.474	1.479 9	1.472 3	1.474	1.488	
C2–O1	1.270	1.254 4	1.275 6	1.292	1.250	1.279
C1–H	1.090	1.082 5	1.090 2		1.090	
O1–H^+	0.980	0.953 3	0.976 2	0.958	1.130	0.986
H^+–O2					1.310	1.688
O2–C5					1.240	1.233
C4–C5						1.490
Bond angles / (°)						
∠C1–C2–C3	122.85				120.37	
∠H^+–O1–C2	114.35	115.8	112.7		118.01	114.5
∠O2–H^+-O1					178.16	
∠C5–O2–H^+					122.81	
Dihedral angles / (°)						
∠O1–C1–C2–C3	–179.76				–179.95	
∠H^+–O1–C2–C3	2.00	2.1	2.2		1.71	
∠O2–C5–C6–C4					179.91	

[a]data from Ref. [40];
[b]data from Ref. [41].

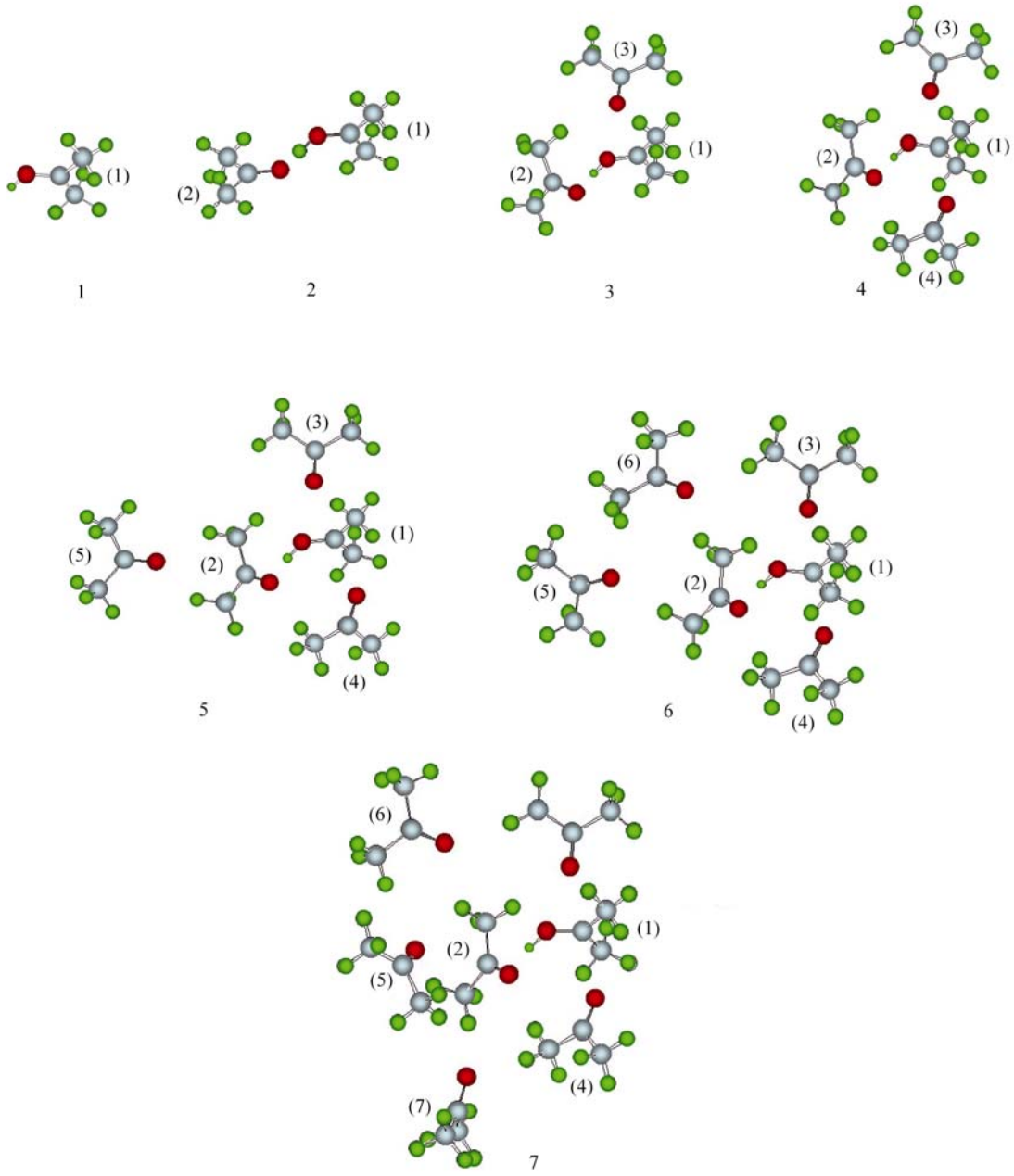

Fig. 9 The optimized equilibrium geometries of the protonated acetone clusters $(CH_3COCH_3)_n H^+$ (n = 1–7) at the B3LYP/ 6231G (d) level.

6 Summary

As the simplest aliphatic ketone, acetone is of interest for molecular reaction dynamics since it plays an important role in photochemistry and environmental science. Our work is concentrated on its isomerization and aggregation to obtain the detailed information on the reaction such as the pathways, the products and their structures, and the growth regularity of clusters. Experimentally, we use the laser ionization mass spectrometer to find the evidences on structural change of acetone molecule and the stability of acetone molecular clusters. Theoretical analysis is based on the DFT/B3LYP method. Various isomerization channels of acetone have been established. The optimal structures of the neutral clusters $(CH_3COCH_3)_n$ and the protonated acetone clusters $(CH_3COCH_3)_n H^+$ for $n = 1-7$ have been determined. The methods employed and the mechanism presented here are general and can be used for measuring and interpreting rearrangement of atoms/molecules in isomerization and aggregation of other organic molecules.

Acknowledgements The work was supported by the National Natural Science Fundation of China (Grant Nos.19925416, 10374036, and 10404008), Chinese Academy of Engineering Physics, and National Education Ministry of China.

References

1. Zare R. -N., Science, 1998, 279: 1875
2. Casavecchia P., Reports on Progress in Physics, 2000, 63: 355
3. Simons J. -P., Comments on Atomic and Molecular Physics, 1985, 16 (3): 157
4. Lifshitz C., Chemical Society Reviews, 2001, 30: 186
5. Valentini J. -J., Annual Review of Physical Chemistry, 2001, 52: 15
6. Aloisio S., and Francisco J. -S., Chem. Phys. Lett., 2000, 329: 179
7. Donaldson D. -J., Gaines G. - A., and Vaida V., J. Phys. Chem., 1988, 92: 2766
8. Trikoupis M. -A., Burgers P. -C., Ruttink P. - J. -A., and Terlouw J. K., Int. J. Mass Spectrom., 2002, 217: 97
9. Liu D., Fang W. -H., and Fu X. -Y., Chem. Phys. Lett., 2000, 325: 86
10. Gierczak T., Burkholder J. -B., Bauerle S., and Ravishankare A. -R., Chem. Phys., 1998, 231: 229
11. Kanomata I, Bull. Chem. Soc. Jpn., 1961, 34: 1864
12. Mouvier G., and Hernndez R., Org. Mass. Spectrom., 1975, 10: 958
13. Hurzeler H, Inghram M. -G., and Morrison J. -D., J. Chem. Phys., 1958, 28: 76
14. Trott W. -M., Blais N. -C., and Walter E. -A., J. Chem. Phys., 1978, 69: 3150
15. Gaines G. -A., Donaldson D. - J., Strickler S. -J., and Vaida V., J. Phys. Chem., 1988, 92: 2762
16. Wei L., Yang B., Yang R., Huang C., Wang J., Shan X., Sheng L., Zhang Y., Qi F., Lam, C. -S., and Li, W. -K., J. Phys. Chem. A, 2005, 109: 4231
17. Zhang X. -K., Parnis J. -M., Lewars E. -G., and March R. -E., Can. J. Chem., 1997, 75: 276
18. Majumder C., Jayakumar O. D., Vatsa R. K., Kulshreshtha K., and Mittal J. -P., Chem. Phys. Lett., 1999, 304: 51
19. Lifshitz C., and Tzidony E., Int. J. Mass Spectrom. Ion. Phys., 1981, 39: 181
20. Majumder C., Jayakumar O. -D., Vatsa R. -K., Kulshreshtha S. -K., and Mittal J. -P., Chem. Phys. Lett., 1999, 304: 51
21. Farmanara Stert P. -V., and Radloff W., Chem. Phys. Lett., 2000, 320: 697
22. Buzza S. -A., Snyder E. -M., Card D. -A., Folmer D. -E., and Castleman Jr. -A. -W., J. Chem. Phys., 1996, 105: 7425
23. Buzza S. -A., Snyder E. -M., and Castleman Jr. -A. -W., J. Chem. Phys., 1996, 104: 5040
24. Lee E. -P. -F., and Dyke H. -M., J. Chem. Faraday Trans., 1992, 88: 2111
25. Aviyente V., and Vernali T., J. Mol. Struct. (Theochem), 1992, 277: 285
26. Ziegler T., Chem. Rev., 1991, 91: 651
27. Valle C. -P., and Novoa J. -J., Chem. Phys. Lett., 1997, 269: 401
28. Perdew J. -P., and Wang Y., Phys. Rev. B, 1992, 45: 13244
29. Becke A. -D., J. Chem. Phys., 1988, 88: 1053
30. Lee C., Yang W., and Parr R. -G., Phys. Rev. B, 1988, 37: 785
31. Hu Z., Jin M. -X., Liu H., and Ding D. -J., Nucl. Phys. Rev., 2002, 19: 188 (in Chinese)
32. Burgers P. -C., Holmes J. -L., Szulejko J. -E., and Mommers A. -A., Org. Mass. pectrom., 1983, 18: 254
33. Dubnikova F., and Lifshitz A., J. Phys. Chem. A, 2000, 104: 4489
34. Hu Z., Jin M. -X., Liu H., and Ding D. J., in The Fifth Asian International Seminar on Atomic and Molecular Physics (Oct. 2－5, 2002, Nara, Japan)
35. Xu X. -S., Hu Z., Jin M. -X., Liu H., and Ding D-J., J. Mol. Struct. (Theochem), 2003, 638: 215
36. Scott A. -P. and Radom L., J. Phys. Chem., 1996, 100: 16502
37. Castleman Jr. -A. -W., Wei S., Annu. Rev. Phys. Chem. 1994, 45: 685; Wei, S., Purnell, J., Buzza S. -A., and Castleman Jr A. W., J. Chem. Phys., 1993, 99: 755
38. Mitchell P., Annu. Rev. Biochem., 1977, 46: 996
39. Yoshino R., Hashimoto K., Omi T., Ishiuchi S., and Fujii M., J. Phys. Chem. A, 1998, 102: 6227
40. Manninen M., Phys. Rev. B, 1986, 34: 6886
41. Boustani I., Chem. Phys. Lett., 1995, 240: 135
42. BelBruno J. -J., Chem. Phys. Lett., 1999, 313: 795
43. Sadlej J., Chem. Phys. Lett., 2001, 333: 485
44. Grönbeck H., and Rosén A., J. Chem. Phys., 1997, 107: 10620
45. Hu Z., Jin M. -X., Xu X. -S., Liu H., and Ding D. -J., J. Chem. J. Chinese Univ., 2003, 24: 671
46. Choo K. -Y., Shinohara H., and Nishi N., Chem. Phys. Lett., 1983, 95: 102
47. Shinohara H., Nagashima U., and Nishi N., Chem. Phys. Lett., 1984, 111: 511
48. Xia P., and Garvey J. -F., J. Phys. Chem., 1995, 99: 3448
49. Lee S. -Y., Shin D. -N., Cho S. -G., and Jung K. -H., J. Mass Spectrom., 1995, 30: 969
50. Xu X. -S., Hu Z., Jin M. X., Liu H., and Ding D. -J., Nucl. Phys. Rev., 2002, 19: 227
51. Xu X. -S., Hu Z., Jin M. -X., Liu H., and Ding D. -J., Chin. J. Chem. Phys., 2004, 17: 21
52. Xu X. -S., Hu Z., Jin M. -X., Liu H., and Ding D. -J., J. At. Mol. Phys., 2005, 22: 585
53. Schlegel H. -B., J. Compu. Chem., 1982, 3: 214
54. Mirkin N. -G., and Krimm S., J. Phys. Chem., 1993, 97: 13887
55. Scott A. -P., and Radom L., J. Phys. Chem., 1996, 100: 16502
56. Xantheas, S. -S., and Dunning Jr. -T. -H., J. Chem. Phys., 1993, 99: 8774
57. Hu Z., Xu X. -S., Jin M. -X., Liu H., and Ding D. -J., in XII International Symposium on Small Particles and Inorganic Clusters (Sept. 6－9, 2004, Nanjing, China)
58. Hirao K., Sano M., and Yamabe S., Chem. Phys. Lett., 1982, 87: 181